The Role of a More Invasive Phenotype in Response to MAPK-Directed Therapies in Thyroid Cancer

Hannah M Hicks[1], Logan R McKenna[1,2], Elise S Bales[1], Veronica L Espinoza[1], Nikita Pozdeyev[1,3], Rebecca E Schweppe[1,2]

[1]Division of Endocrinology, Metabolism, and Diabetes, Department of Medicine, University of Colorado Anschutz Medical Campus, Aurora, CO.

[2]University of Colorado Cancer Center, University of Colorado Anschutz Medical Campus, Aurora, CO.

[3]Division of Bioinformatics and Personalized Medicine, Department of Medicine, University of Colorado Anschutz Medical Campus, Aurora, CO.

Department of Medicine Research Day 2022

Abstract

Purpose: Advanced papillary thyroid cancer (PTC) and anaplastic thyroid cancer (ATC) are the leading causes of endocrine cancer death. Mutations in the MAP kinase (MAPK) pathway are common in PTC and ATC, especially in *BRAF,* with a prevalence of 40-60%. *BRAF*-mutant PTC patients currently lack targeted therapeutic options, and despite the approved combination of BRAF and MEK inhibition for patients with *BRAF*-mutant ATC, these patients often progress.

Results: An emerging mechanism of resistance to targeted therapies is an invasive phenotype switch in which cells transition from a proliferative, therapy sensitive population to an invasive, therapy resistant population. This phenotype has been studied in response to BRAF inhibition in melanoma but has yet to be characterized in thyroid cancer. Here, we sought to determine whether increased invasion plays a role in resistance to BRAF inhibition in *BRAF*-mutant PTC and ATC.

In our panel of *BRAF*-mutant PTC and ATC cell lines with varying sensitivity/resistance to the BRAF inhibitor dabrafenib (BRAFi), we showed that cells resistant to BRAFi exhibit a 1.8 to 2.2 fold increase ($p<0.04$) in invasion while sensitive cells do not. We further found that conditioned media from BRAFi-treated resistant cells promotes invasion 3.8 to 5.7-fold ($p<0.0048$). Using RPPA, we identified a 2.0-fold increase in the extracellular matrix protein, fibronectin (FN), in response to BRAFi treatment and identified a 1.6 to 3.2 fold increase ($p<0.02$) in FN secretion in resistant cell lines. Accordingly, treatment with FN phenocopies BRAFi-treatment by increasing invasion 1.9 to 2.1 fold ($p<0.04$), and depletion of FN results in loss of increased invasion. Resistant cells with depleted FN also fail to exhibit BRAFi-induced increase in secreted FN.

MAPK pathway reactivation is a common mechanism of resistance to inhibitors of the MAPK pathway, which we have shown can be blocked by dual BRAF and ERK inhibition (Hicks, HM; McKenna, LR *et al.* Mol Carcinog. 60(3) 2021). ERK inhibition also mitigates the increase in invasion observed in response to single-agent BRAFi or FN in resistant cells. We further observed that dual inhibition of BRAF and ERK decreases circulating FN and slows tumor growth *in vivo* in a BRAFi-resistant patient-derived xenograft model ($p=0.02$). Finally, using RNA-sequencing followed by ChIP Enrichment Analysis, we identified a down-regulation of EGR1 transcript levels and transcriptional targets in response combined BRAF/ERK inhibition compared to single-agent BRAFi alone.

Conclusions: These data indicate that thyroid cancer cells resistant to BRAF inhibition exhibit a more invasive phenotype characterized by an increase in FN and a pro-invasive secretome. Dual inhibition of BRAF and ERK ablates this BRAFi-driven increase in invasion and slows tumor growth *in vivo,* providing a potential therapeutic strategy for *BRAF*-mutant thyroid cancer patients.

Introduction

An invasive phenotype is an emerging mechanism of resistance to targeted therapies[1,2]

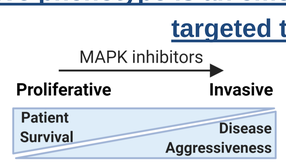

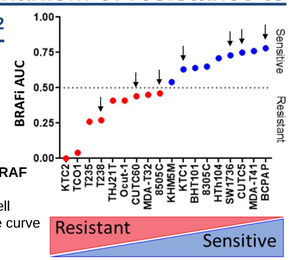

Figure 1. ***BRAF*-mutant thyroid cancer cell lines exhibit varying sensitivity to BRAF inhibition[3].** A panel of 18 thyroid cancer cell lines with *BRAF*-V600E mutations were treated with increasing concentrations of dabrafenib (BRAF inhibitor) for 72 hours. Cell viability was measured using CellTiter-Glo 2.0 assays. Area under the dose response curve (AUC) values were calculated with greater AUC signifying greater sensitivity (arrows indicate cell lines chosen for future studies).

BRAF inhibition promotes invasion and a pro-invasive secretome

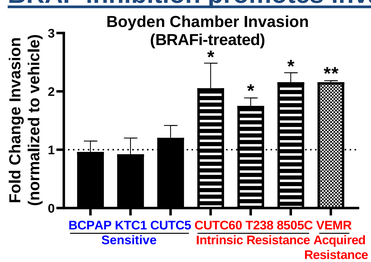

Figure 2. BRAF inhibition increases invasion in cell lines with intrinsic or acquired resistance. *BRAF*-V600E cell lines that are sensitive (BCPAP, KTC1, CUTC5), have acquired resistance (KTC1-VEMR)[4], or intrinsic resistance (CUTC60, T238, 8505C) to BRAF inhibition were treated with dabrafenib (BRAFi, 100 nM) for 24 hrs then plated in Matrigel-coated Boyden chambers for 24 hrs. Invading cells were stained with DAPI, counted using ImageJ, and normalized to growth. Results displayed as mean normalized to vehicle-treated control, +/- SEM. *, $p<0.05$; **, $p<0.01$.

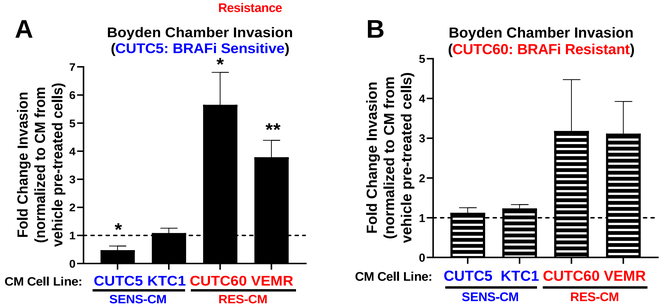

Figure 3. Conditioned media from resistant, but not sensitive, cells is pro-invasive. A) BRAFi-sensitive or **B)** -resistant cell lines were treated with conditioned media from indicated cell lines (listed on the x-axis), which were pre-treated with either vehicle or BRAFi (100 nM) for 24 hrs then plated in Matrigel-coated Boyden chambers for 24 hrs, stained with DAPI, counted using ImageJ, and normalized to growth. Results displayed as mean normalized to vehicle-treated control (i.e. invasiveness of cells treated with CM from a vehicle-treated cell line) +/- SEM. *, $p<0.05$; **, $p<0.01$.

Results

Cellular and secreted fibronectin are increased in response to BRAF inhibition

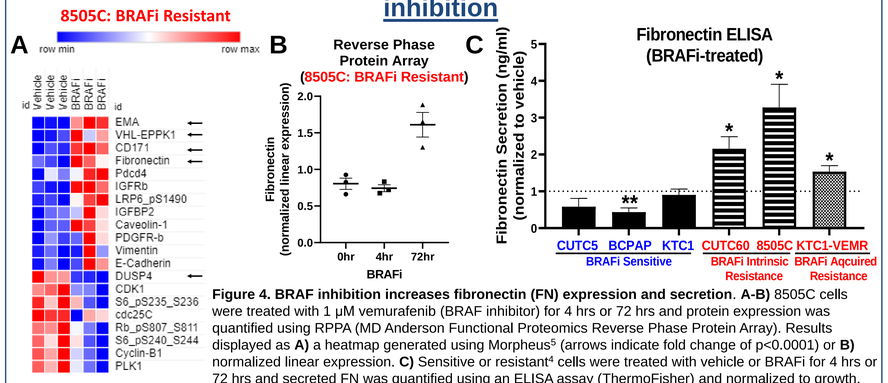

Figure 4. BRAF inhibition increases fibronectin (FN) expression and secretion. A-B) 8505C cells were treated with 1 μM vemurafenib (BRAF inhibitor) for 4 hrs or 72 hrs and protein expression was quantified using RPPA (MD Anderson Functional Proteomics Reverse Phase Protein Array). Results displayed as **A)** a heatmap generated using Morpheus[5] (arrows indicate fold change of $p<0.0001$) or **B)** normalized linear expression. **C)** Sensitive or resistant[4] cells were treated with vehicle or BRAFi for 4 hrs or 72 hrs and secreted FN was quantified using an ELISA assay (ThermoFisher) and normalized to growth. *$p<0.05$; **$p<0.01$.

Hypothesis: BRAF inhibition increases invasion in resistant cells via fibronectin and a pro-invasive secretome.

Fibronectin is required for an invasive phenotype

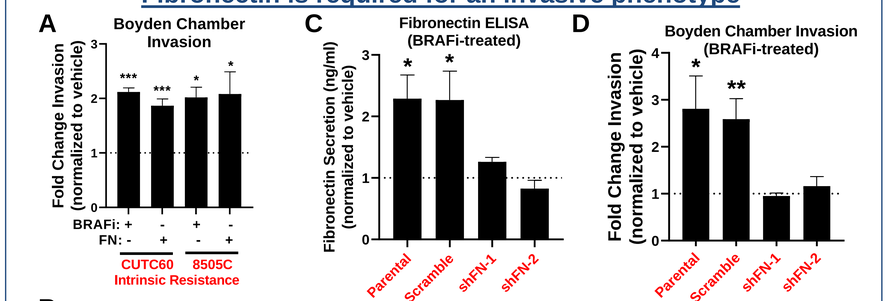

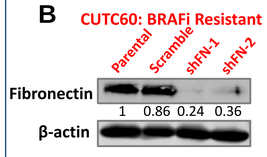

Figure 5. FN is required for a BRAFi-induced invasive phenotype. **A)** BRAFi-resistant cells were treated with FN (100 ng/ml) or BRAFi (100 nM) for 24 hrs than plated in Matrigel-coated Boyden chambers for 24 hrs. Invading cells were stained with DAPI and counted using ImageJ. **B)** FN was knocked down using shRNA in CUTC60 cells. Cell lysates were analyzed via Western Blot for the indicated antibodies. **C)** Cells were treated with vehicle or BRAFi for 72 hrs and secreted FN was quantified using an ELISA assay (ThermoFisher). **D)** Indicated cells were treated with BRAFi for 24 hrs then plated in Matrigel-coated Boyden chambers for 24 hrs. Invading cells were stained with DAPI, counted using ImageJ, and normalized to growth. Results displayed as mean normalized to vehicle-treated control +/- SEM. *, $p<0.05$; **, $p<0.01$.

Combined BRAF and ERK1/2 inhibition can block an invasive phenotype

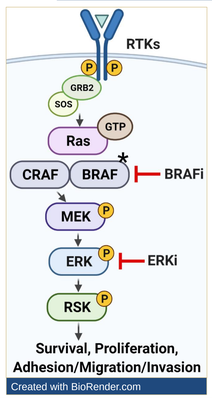

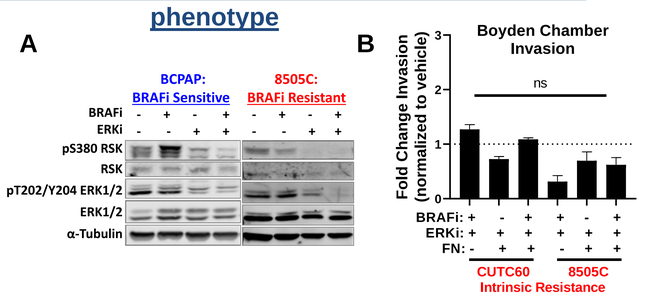

Figure 6. Combined BRAFi/ERKi prevents MAPK pathway reactivation and invasion. A) BRAFi-sensitive and -resistant cells were treated with BRAFi (50 nM), ERKi (1), or the combination at various time points. Cell lysates were analyzed via western blot with the indicated antibodies. **B)** BRAFi resistant cells were treated with indicated compounds for 24 hrs then plated in Matrigel-coated Boyden chambers for 24 hrs. Invading cells were stained with DAPI, counted using ImageJ, and normalized to growth.

Results

Combined BRAF and ERK1/2 inhibition slows tumor growth and inhibits fibronectin *in vivo*

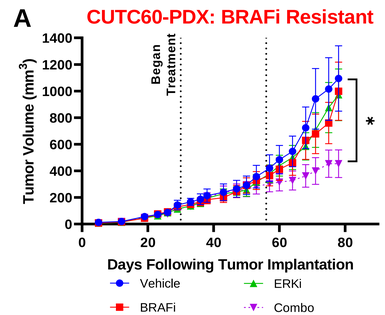

Figure 7. Combined BRAF and ERK inhibition reduces tumor growth and circulating FN *in vivo*. A) Patient-derived xenograft (PDX) tumor chunks were injected into the flanks of athymic nude mice. Once tumors reached an average of 100mm^3, treatment with vehicle, BRAFi, ERKi, or the combination was performed via oral gavage once daily. At day 55 post-injection, doses of BRAFi and ERKi were increased. **B)** At the time of sacrifice, plasma was isolated from blood samples. FN ELISA assays (Abcam) were performed to measure circulating FN. *, $p<0.05$. BRAFi: dabrafenib (30 mg/kg prior to day 55, 50 mg/kg post); ERKi: BVD-523 (50 mg/kg prior to day 55, 100 mg/kg post).

Combined BRAF and ERK1/2 inhibition decreases EGR1 transcript levels and transcriptional targets

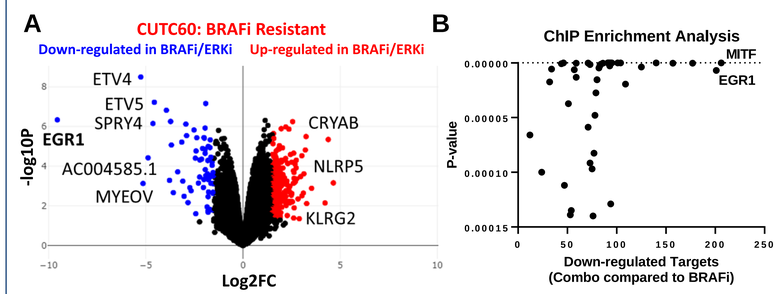

Figure 8: Combined BRAF and ERK1/2 inhibition decreases EGR1 transcript levels and transcriptional targets. A-B) RNA-sequencing was performed on CUTC60 cells treated with BRAFi (100 nM), ERKi (1 μM) or the combination for 48 hrs (Anschutz Medical Campus Functional Genomics Core) and analyzed using BioJupies[6] to **A)** generate a volcano plot and **B)** perform ChIP Enrichment Analysis (ChEA).

Conclusions

Conclusions:

- BRAF inhibition promotes invasion through a pro-invasive secretome in BRAF-inhibitor resistant thyroid cancer cells
- FN phenocopies BRAFi by increasing invasion and is required for a BRAF inhibitor-induced invasive phenotype
- Combined BRAF and ERK1/2 inhibition decreases invasion *in vitro* and inhibits tumor growth and circulating FN *in vivo*
- Combined BRAF and ERK1/2 inhibition decreases EGR1 transcript levels and transcriptional targets

Disclosures: The authors have no conflicts of interest to disclose.

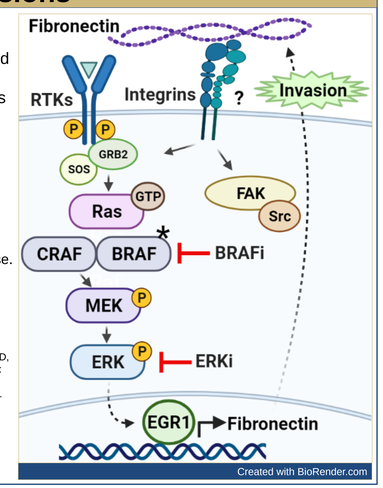

References:

1. Kemper K, de Goeje PL, Peeper DS, van Amerongen R. Cancer Res. 2014 Nov 1;74(21):5937-41. doi: 10.1158/0008-5472.CAN-14-1174. Epub 2014 Oct 15. **PMID: 25320006**
2. Li FZ, Dhillon AS, Anderson RL, McArthur G, Ferrao PT. Front Oncol. 2015 Feb 13;5:31. doi: 10.3389/fonc.2015.00031. **PMID: 25763355**
3. Hicks HM, McKenna LR, Espinoza VL, Pozdeyev N, Pike LA, Sams SB, LaBarbera D, Reigan P, Raeburn CD, E Schweppe R. Mol Carcinog. 2021 Mar;60(3):201-212. doi: 10.1002/mc.23284. **PMID: 33595872**
4. Danysh BP, Rieger EY, Sinha DK, Evers CV, Cote GJ, Cabanillas ME, Hofmann MC. Oncotarget. 2016 May 24;7(21):30907-23. doi: 10.18632/oncotarget.9023. **PMID: 27127178**
5. Morpheus, https://software.broadinstitute.org/morpheus
6. Torre D, Lachmann A, Ma'ayan A. Cell Syst. 2018 Nov 28;7(5):556-561.e3. doi: 10.1016/j.cels.2018.10.007. Epub 2018 Nov 14. **PMID: 30447998**

Funding: 1F31CA257079-01A1, 5R01CA22229-03